Synthesis and photoluminescence of nano/ microstructured $Y_{0.95}Eu_{0.05}PO_4$ via hydrothermal process

JINRONG BAO*, YUE LU, WENXIAN LI, HUA WANG, RANBO YU[a]
School of Chemistry and Chemical Engineering, University of Inner Mongolia, Hohhot 010021, China,
[a]Department of Physical Chemistry, University of Science and Technology Beijing, Beijing 100083, China

The nano/microstructured $Y_{0.95}Eu_{0.05}PO_4$ have been hydrothermally synthesized by changing the pH value and PO_4/RE molar ratio. The structures and morphologies of the as-synthesized $Y_{0.95}Eu_{0.05}PO_4$ have been investigated by X-ray powder diffraction (XRD), thermogravimetric analysis (TGA) and field-emission scanning electron microscopy (FE-SEM). The results indicate that the small nanoparticals formed at lower pH value and the microparticals obtained at higher pH value. A possible formation mechanism of the products was also proposed. The luminescent properties of the products prepared with different pH values have been studied. When the pH value from 1.0 to 8.0, the products of luminescence intensity was decreased.

(Received February 21, 2013; accepted January 22, 2014)

Keywords: Rare earth phosphate, Nano/microstructure, Luminescence

1. Introduction

Rare earth orthophosphates ($REPO_4$), a family of important phosphate compounds, have been studied intensively based on their special physical and chemical properties from their 4f electrons [1-5]. Rare earth orthophosphates $REPO_4$ have a variety of potentially beneficial properties, including high thermal stability with melting points up to 2300 °C [6], high index of refraction, high concentration of lasing ions [7], low toxicity, high luminescence quantum yield, and sharp emission bands. These properties provide the basis for their use in a wide range of applications such as luminescence or laser materials, moisture sensors, heat-resistant materials, and nuclear waste disposal [8-10].

Very recently, rare earth compounds and lanthanide-doped compounds nanowires with interesting optical properties have been successfully prepared [2,11,12]. By using the surfactant-assisted process, the $CePO_4$ and $CePO_4$:Tb nanowires with a narrow diameter distribution and uniform morphology could be hydrothermally synthesized [13]. Furthermore, $REPO_4$ and $REPO_4:Ln^{3+}$ nanocrystal with narrow size dispersion and good optical properties have been obtained by using a high-boiling-solvent technique [14,15]. Luminescent $LaPO_4$:Ce,Tb nanoparticles with high quantum yield were recently prepared using a microwave-assisted synthesis method with some ionic liquids as the reaction media [16].

Controlling the shape and size of phosphor particles are fundamental to fulfill their various applications. For example, uniform spherical particles in the sub-micrometer size range are preferred in the applications of fluorescent lamps and PDP (please define PDP at its first use) devices [17,18]. It has been also established that the nanowires with smooth, highly uniform morphologies and high aspect ratio may lead to significant photoluminnescent enhancement [19]. The controllability in synthezing phosphors with uniform morphology and tunable particle size and shape is also highly desired for fundamental studies dealing with the effects of these morphological characteristics on the luminescence efficiency, which still remains unclear [20,21]. Different kinds of YPO_4 nano/microcrystals have been synthesized by chemical methods [2,11,12,16,22-26]. However, there are few reports on controlled synthesizing YPO_4 particles with narrow size distribution from nanometer to micrometer, which limited the understanding and investigating on optimum size of YPO_4 particles in the applications of luminescence lamps and PDP devices. Herein, we developed a simple hydrothermal route to synthesize uniform nano/microstructured $Y_{0.95}Eu_{0.05}PO_4$. The products $Y_{0.95}Eu_{0.05}PO_4$ crystal particles are from nanometer to micrometer by adjusting the solutions pH value and PO_4/RE molar ratio. The dependence of the photoluminescent properties on the sizes of the products and pH value was investigated.

2. Experimental section

All the chemicals (AR grade) were purchased from Beijing Chemical Reagent Company. They were used without any further treatment. Europium nitrate stock

solutions were prepared by dissolving Eu_2O_3 in dilute HNO_3 solution at elevated temperature with agitation. .

In a typical synthesis, 0.95 moL $Y(NO_3)_3$ and 0.05 moL $Eu(NO_3)_3$ mixed solution was added slowly to 1 mol/L phosphoric acid (10 mL) solution under stirring and keeping PO_4/RE molar ratio was 10. Then the pH value of as-obtained transparent solution was adjusted from 1.0 to 8.0, respectively, by adding ammonia (25 %), and was quickly transferred into a stainless steel autoclave with inner Teflon vessel (volume, 50 mL). The autoclave was sealed and maintained at 180 °C for 12 h. Then the autoclave was naturally cooled to room temperature. The resulting white solid precipitates were filtered, washed three times with deionized water. At last, the products were washed with absolute alcohol before drying at 60 °C for 8 h. For clarity, $Y_{0.95}Eu_{0.05}PO_4$ products synthesized at pH value of 1.0, 4.0, 6.0, 8.0 were described in this paper.

The phase composition of the samples was identified by X-ray diffraction (Model M21XVHF22, MAC science Co., Ltd., Japan) using Cu Kα radiation in the range of 10–60° at room temperature. Thermogravimetric analysis(TGA) of powders performed up to 700 °C at the heating rate of 10 °C/min under air flow (TGA instrument, model Q50V20.6 Build 31). Morphologic studies were performed by field-emission scanning electron microscopy (FE-SEM, LEO1530). The luminescence spectra of powders were collected in F-4500 FL Spectrophotometer at room temperature.

3. Results and discussion

The typical XRD patterns of the products prepared without doped Eu^{3+} (pH= 1.0) and 5 % Eu^{3+} doped YPO_4 with different pH value (pH= 1.0, 4.0, 6.0, 8.0) were shown in Fig. 1a-e. All the powders give rise to single-phase and well crystallized $Y_{0.95}Eu_{0.05}PO_4$ as identified by XRD analysis. The diffraction peaks agree well with a tetragonal structure YPO_4 [space group I41 (140), PDF card no 74-2429]. No additional peaks were detected, implying that a doping with Eu^{3+} ions did not lead to the modification of the YPO_4 host crystal structure.

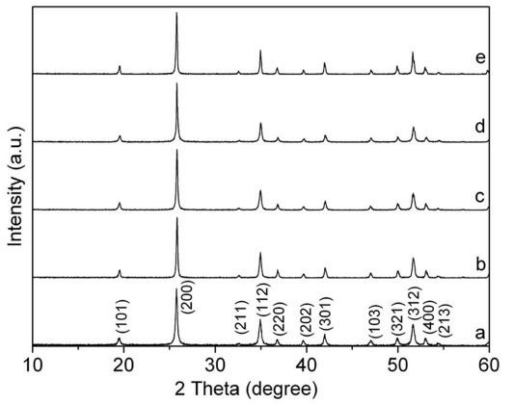

Fig. 1. XRD patterns of products (a) YPO_4 prepared with pH=1.0 and (b-e) $Y_{0.95}Eu_{0.05}PO_4$ prepared with different pH values (pH=1.0, 4.0, 6.0, 8.0).

Typical TGA plots further confirmed the hydrated nature of the derived as-synthesized $Y_{0.95}Eu_{0.05}PO_4$ products (Fig. 2). All the TGA plots of these samples show a weight loss occur in two steps from 40 to 600 °C. The first one occurs in the temperature range 60 ～ 150 °C, and is associated with the release of residual water and chemical adsorbed water adsorbed on the powder surface in air condition. The two weight loss process is slower up to 600 °C, which is attributed to the decrease or removal of the synthesis residuals and adsorptions such as NO_3^- and OH^- [24]. The weight losses were 4.58%, 5.68%, and 5.97% for the products prepared with pH values of 1.0, 4.0, and 6.0, respectively.

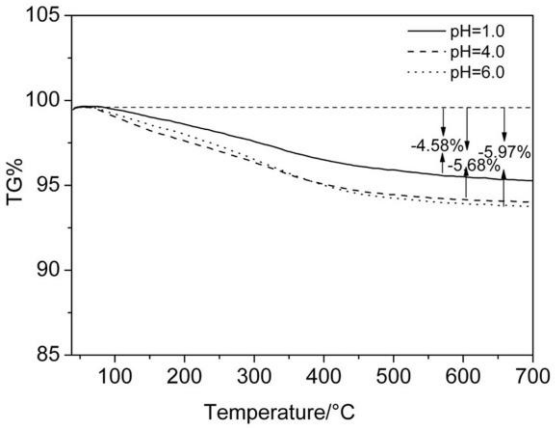

Fig. 2. TG plots of as-synthesized $Y_{0.95}Eu_{0.05}PO_4$ with different pH values of: (a) pH=1.0, (b) pH=4.0, (c) pH=6.0.

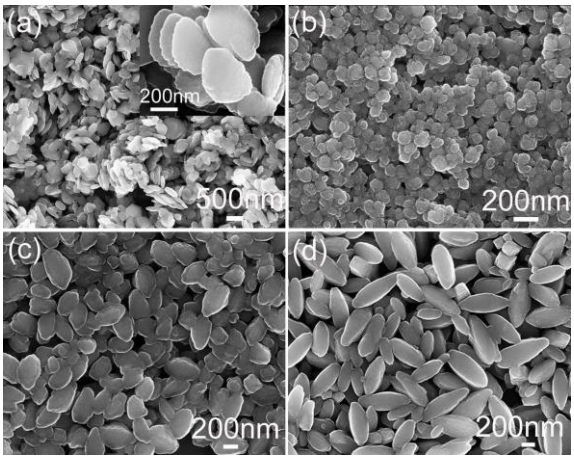

Fig. 3. FE-SEM images of the as-synthesized $Y_{0.95}Eu_{0.05}PO_4$ with different pH values of: (a) pH=1.0, (b) pH=4.0, (c) pH=6.0, (d) pH=8.0.

Morphological studies by FE-SEM demonstrate that the pH value plays an important role in both modulating the morphology and particle size of the $Y_{0.95}Eu_{0.05}PO_4$ crystal (Fig. 3). As shown in Fig. 3a, when the pH value is 1.0, the formed $Y_{0.95}Eu_{0.05}PO_4$ consists of nanodishes with a homogeneous thickness 50 nm ～ 60 nm and diameter

300 nm ～ 400 nm distribution. With the pH value increasing to 4.0, sphere-like particles were obtained, which are about 100 nm in diameters (Fig. 3b). As increasing the pH value to 6.0, the as-synthesized $Y_{0.95}Eu_{0.05}PO_4$ exhibits a quasi-shuttle like morphology with an average diameter of about 200 nm ～ 300 nm (Fig. 3c). When the pH value was further increased to 8.0, the product was uniform shuttle-like with lengths about 1 μm and diameters about 300 nm～400 nm (Fig. 3d).

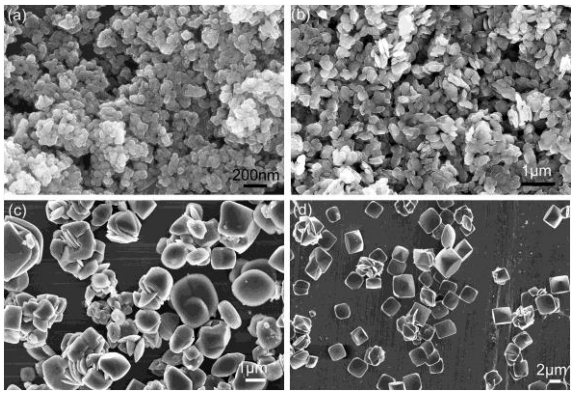

Fig. 4. FE-SEM images of the products prepared with different reactant PO_4/RE molar ratios of: (a) 1.0, (b) 10, (c) 60, (d) 120.

In order to further understand the formation process of the products morphologies and sizes, controlled experiments were carried out to investigate the influence the reactant PO_4/RE molar ratio and the pH value on the synthesis of $Y_{0.95}Eu_{0.05}PO_4$ samples. When the reactant PO_4/RE molar ratio is 1.0, without ammonia (25 %), an inhomogeneous nanoparticals were obtained (Fig. 4a), which are about 50 ～ 60 nm in diameter. When the reactant PO_4/RE molar ratio increased to 10, the product is composed of nanodishes with thickness 50 nm ～ 60 nm and diameter 300 nm ～ 400 nm (Fig. 4b). The reactant PO_4/RE molar ratio is 60, the majority morphologies were octahedron-like microstructures and dishes-like particles (Fig 4c). Furthermore, when the reactant molar ratio PO_4/RE increasing to 120, the corresponding morphology dramatically appears as uniform octahedron-like microstructures with a width of about 2 ～ 3 μm (Fig. 4d). When the reactant PO_4/RE molar ratio is 10, and the pH values were adjusted from 1.0 to 8.0 by adding ammonia (25 %), YPO_4 nano/microparticals was obtained (Fig. 3). Generally, hexagonal $LnPO_4$ tend to grow as 1D nanowires, which is possibly due to the 1D characteristics of the infinite linear chains of hexagonal structured $LnPO_4$ (Ln = La–Dy). On the contrary, tetragonal (Ho-Lu, Y)PO_4 has no preferred growth direction in the crystalline phase based on their crystal structure. Therefore, the resulting irregularly shaped particle morphology can also be obtained [11]. In our case, phosphoric acid is excessive. With the reactant PO_4/RE molar ratio increasing, the supersaturation of the solution was increase. It is quite possible that excessive PO_4^{3-} are absorbed on the surface of the initially formed tiny $REPO_4$ particles at the early stage of the reactions, due to the strong interactions between the RE^{3+} and the PO_4^{3-} on the particle surface [27,28]. When phosphoric acid is excessive, the electrostatic potential on the crystal surfaces of initial $REPO_4$ particles will increase [29,30]. To minimize surface energy [31], these nanoparticles might assembly and crystallize into octahedron-like microstructures. When the PO_4/RE molar ratio was 10, ammonia (25 %) are used to adjust the pH value, the ammonia reacts with the excessive H_3PO_4 to form $NH_4H_2PO_4$ at early stage of the reaction, which will then react with Y^{3+}(Eu^{3+}) to form $Y_{0.95}Eu_{0.05}PO_4$. The formation of $NH_4H_2PO_4$ could decrease crystallization velocity of the product, and might be useful in controlling the growth and aggregation of $Y_{0.95}Eu_{0.05}PO_4$ particles. Moreover, considering the different morphologies maybe the different cation ions (H^+, NH_4^+) in the reaction solution correspond to it [32].

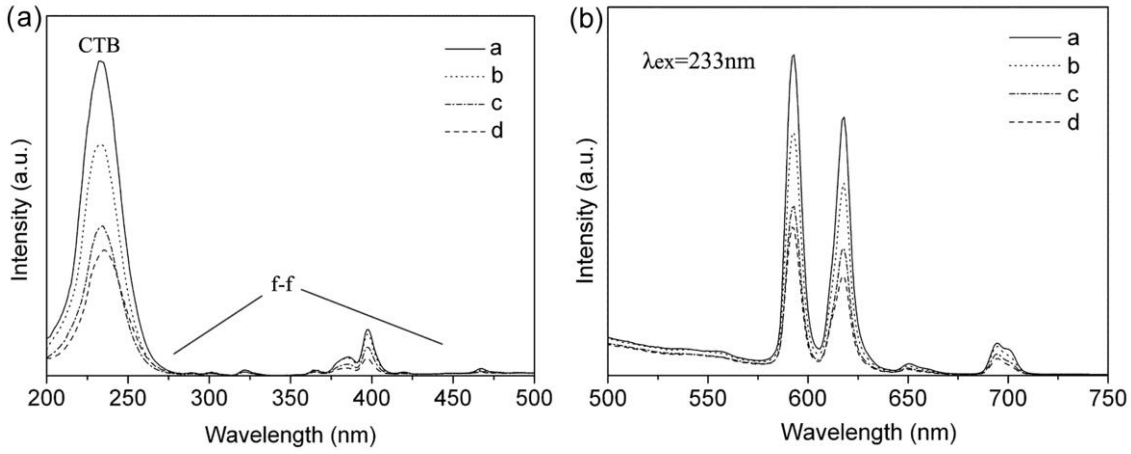

Fig. 5. (a) Excitation spectrum and (b) emission spectrum of the solid products obtained at different pH value of: a pH=1.0, b pH=4.0, c pH=6.0, d pH=8.0.

The room-temperature luminescence spectra were recorded for solid products of different pH values (Fig. 5). The excitation spectra of the products centered at 233 nm, which is assigned to the oxygen-europium charge transfer process (Fig. 5(a)). In addition, a broad peak extending from 300 to 475 nm due to the direct excitation of the Eu^{3+} ground state into higher levels of the 4f-manifold such as $^7F_0$–$^5L_6$ at 395 nm was also exhibited. The emission spectrum excited at 233 nm was also recorded as shown in Fig. 5(b). The emission spectra consist of sharp peaks at about 592, 617, 650, 696 nm, which are assigned to the transitions of $^5D_0\rightarrow{}^7F_1$, $^5D_0\rightarrow{}^7F_2$, $^5D_0\rightarrow{}^7F_3$, $^5D_0\rightarrow{}^7F_4$, respectively [33]. Although the major peaks in the emission spectrum are identical for $Y_{0.95}Eu_{0.05}PO_4$ products synthesized at different pH value, the luminescence intensity are different. Interestingly, the nanodishes of $Y_{0.95}Eu_{0.05}PO_4$ synthesized at pH of 1.0 exhibit the strongest emission intensity. With the pH value increasing, the emission intensity of products was decreased. The difference in luminescence properties is possibly ascribed to the sizes of the products and hydroxyl quenching due to the presence of some adsorbate during the synthesis of the products [34]. This hydroxyl quenching result is also in agreement with the TG results. As described in the above, the different amount of surface adsorbed water and OH^- will result in different luminescence properties.

4. Conclusions

In summary, nano/microsized $Y_{0.95}Eu_{0.05}PO_4$ with controlled morphology and size can be synthesized by adjusting the PO_4/RE molar ratio and pH value with ammonia. The reactant PO_4/RE molar ratio is one of the most important factors in our experiment. We proposed that the in-situ-formed $NH_4H_2PO_4$ played an important role in the formation of $Y_{0.95}Eu_{0.05}PO_4$ crystal by decreasing crystallization velocity. The $Y_{0.95}Eu_{0.05}PO_4$ crystals with controlled morphology and size exhibited different luminescence intensity, which might relate to the sizes and the surface hydroxyl effect. This facile hydrothermal approach may provide a feasible approach for manipulating various uniform nano/microstructures with controlled morphologies and interesting optical properties.

Acknowledgment

This work was financially supported by National Natural Science Foundation of China (No. 20871015, 20401015 and 20861005) and National Natural Science Foundation of Inner Mongolia Autonomous Region (No. 2011BS0801).

Reference

[1] G. Y. Adachi, N. Imanaka. Chem. Rev. **98**, 1479 (1998).
[2] R. X. Yan, X. M. Sun, X. Wang, et al. Chem. Eur. J. **11**, 2183 (2005).
[3] S. P. Fricker. Chem. Soc Rev **35**, 524 (2006).
[4] J. Dhanaraj, R. Jagannathan, T. R. N. Kutty, et al. J. Phys. Chem. B **105**, 11098 (2001).
[5] H. Mass, A. Currao, J. Calzaferri. Angew. Chem. Int. Ed. **41**, 2495 (2002).
[6] A. Rouanet, J. J. Serra, K. Allaf, et al. Inorg. Mater. **17**, 104 (1981).
[7] Y. Guo, P. Woznicki, A. Barkatt, et al. J. Mater. Res. **11**, 639 (1996).
[8] O. Lehmann, K. Kompe, M. Haase, J. Am. Chem. Soc. **126**, 14935 (2004).
[9] K. Riwotzki, H. Meyssamy, A. Kornowski, et al. J. Phys. Chem. B **104**, 2824 (2000).
[10] P. Schuetz, F. Caruso. Chem. Mater. **14**, 4509 (2002).
[11] Y. P. Fang, A.W. Xu, R.Q. Song, et al. J. Am. Chem. Soc. **125**, 16025 (2003).
[12] Y. W. Zhang, Z. G. Yan, L. P. You, et al. Eur. J. Inorg. Chem. 4099 (2003).
[13] W. B. Bu, Z. L. Hua, H. R. Chen, et al. J. Phys. Chem. B **109**, 14461 (2005).
[14] K. Riwotzki, H. Meyssamy, H. Schnablegger, et al. Angew. Chem. Int. Ed. **40**, 573 (2001).
[15] K. Kompe, H. Borchert, J. Storz, et al. Angew. Chem. Int. Ed. **42**, 5513 (2003).
[16] G. Buhler, C. Feldmann. Angew. Chem. Int. Ed. **45**, 4864 (2006).
[17] Y. C. Kang, E. J. Kim, D. Y. Lee, et al. Alloys Compd. **347**, 266 (2002).
[18] N. O. Nuñez, S. R. Liviano, M. J. Ocaña. Nuria O. Colloid Interface Sci. **349**, 484 (2010).
[19] J. R. Bao, R. B. Yu, J. Y. Zhang, et al. Scripta Mater. **62**, 133 (2010).
[20] F. Wang, J. Wang, X. Liu. Angew. Chem. Int. Ed. **49**, 7456 (2010).
[21] J. Shan, M. Uddi, N. Yao, et al. Adv. Funct. Mater. **20**, 3530 (2010).
[22] Z. Y. Huo, C. Chen, D. Chu, et al. Chem. Eur. J. **13**, 7708 (2007).
[23] H. Lai, A. Bao, Y. M. Yang, et al. J. Phys. Chem. C **112**, 282 (2008).
[24] W. H. Di, X. X. Zhao, S. Z. Lu, et al. J. Solid State Chem. **180**, 2478 (2007).
[25] Z. Y. Huo, C. Chen, Y. D. Li. Chem. Commun. 3522 (2006).
[26] J. M. Nedelec, D. Avignant, R. Mahiou. Chem. Mater. **14**, 651 (2002).
[27] A. Fillankembo, S. Giorgio, I. Lisiecki, M. P. Pileni, J. Phys. Chem. B **107**, 7492 (2003).

[28] E. Matijevit, R. S. Sapieszko, J. B. Melville, J. Colloid Interface Sci. **50**, 567 (1975).
[29] R. Kern, Crystal Growth and Adsorption, in Growth of Crystals, Ed. N. N. Sheftal, Consultants Bureau. New York, 1969, 8, p. 3.
[30] P. Hartman, Modern PBC theory. In: Morphology of crystals, Part A, Tokyo: Terra Scientific Publishing Company, 1987, 270-319.
[31] R. L. Penn, J.F. Banfield, Science. **281**, 669 (1998).
[32] T. Xia, Q. Li, X. D. Liu, et al. J. Phys. Chem. B **110**, 2006 (2006).
[33] X. Li, H. F. Bi, J. Alloys and Compounds **532**, 72 (2012).
[34] W. H. Di, X. J. Wang, B. J. Chen, et al. J. Phys. Chem.
B **109**, 13154 (2005).

*Corresponding author: jinrongbao@imu.edu.cn